THE ASTROPHYSICAL JOURNAL, 492:267–280, 1998 January 1

NEUTRON STAR MAGNETIC FIELD EVOLUTION, CRUST MOVEMENT, AND GLITCHES

MALVIN RUDERMAN, TIANHUA ZHU, AND KAIYOU CHEN
Physics Department and Columbia Astrophysics Laboratory, Columbia University, 538 West 120th Street, New York, NY 10027
Received 1997 April 25; accepted 1997 August 13

ABSTRACT

Spinning superfluid neutrons in the core of a neutron star interact strongly with coexisting superconducting protons. One consequence is that the outward (inward) motion of core superfluid neutron vortices during spin-down (spin-up) of a neutron star may alter the core's magnetic field. Such core field changes are expected to result in movements of the stellar crust and changes in the star's surface magnetic field that reflect those in the core below. Observed magnitudes and evolution of the spin-down indices of canonical pulsars are understood as a consequence of such surface field changes. If the growing crustal strains caused by the changing core magnetic field configuration in canonical spinning-down pulsars are relaxed by large-scale crust-cracking events, special properties are predicted for the resulting changes in spin period. These agree with various glitch observations, including glitch activity, permanent shifts in spin-down rates after glitches in young pulsars, the intervals between glitches, families of glitches with different magnitudes in the same pulsar, the sharp drop in glitch intervals and magnitudes as pulsar spin periods approach 0.7 s, and the general absence of glitching beyond this period.

Subject headings: dense matter — pulsars: general — stars: magnetic fields — stars: neutron

1. INTRODUCTION

A canonical neutron star consists mainly of superfluid neutrons, superconducting protons (with an abundance a few percent that of the neutrons), and an equal number of relativistic degenerate electrons (Fermi energy $\sim 10^2$ MeV). In the outer kilometer the protons clump into a lattice of neutron-rich nuclei (the stellar "crust") with the neutron superfluid filling the space between. A spinning neutron star's superfluid neutrons rotate at an angular rate Ω only by establishing an array of quantized vortex lines parallel to the stellar spin axis, with an area density

$$n_V = 2m_n\Omega/\pi\hbar \sim 10^4/P(\mathrm{s})\ \mathrm{cm}^{-2}\ . \quad (1)$$

Any magnetic field that passes through the star's superconducting protons must become very inhomogeneously structured. In a type II superconductor, expected to be present below the crust and perhaps all the way down to the central core, the magnetic field becomes organized into

$$n_\Phi = B/\Phi_0 \sim 10^{19}B_{12}\ \mathrm{cm}^{-2} \quad (2)$$

quantized flux tubes per unit area, with

$$\Phi_0 = \pi\hbar c/e = 2 \times 10^{-7} \quad (3)$$

the flux in each tube. Unlike the quasi-parallel neutron vortex line array, the flux-tube array is expected to have a complicated twisted structure following that of the much smoother toroidal plus poloidal magnetic field that existed before the transition into superconductivity (at about 10^9 K).

A spinning-down (spinning-up) neutron star's neutron superfluid vortex array must expand (contract). Because the core of a neutron vortex and a flux tube interact strongly as they pass through each other, the moving vortices will push on the proton's flux-tube array (Sauls 1989; Srinivasan et al. 1990; Ruderman 1991a, 1991b), forcing it either (*a*) to move together with the vortices or (*b*) to be cut through if the flux-tube array cannot respond fast enough to take part in the vortex motion. Section 2 discusses possible relationships among a pulsar's Ω, B, and rate of change of spin ($\dot{\Omega}$), which discriminate between these two behaviors. In case *a* the evolution of the magnetic field at the core-crust interface is well determined by the initial magnetic field configuration and subsequent changes in stellar Ω. In case *b* the core-crust interface field would evolve more slowly relative to changes in Ω, although qualitative features of the evolution should be similar to those of case *a*. Some microphysics and observations, considered in §§ 2 and 3, support case *a* behavior for pulsars whose spin-down (or spin-up) ages, $T_s = |\Omega/2\dot{\Omega}|$, are not less than those of Vela-like radio pulsars ($T_s \sim 10^4$ yr) and case *b* behavior for the much more rapidly spinning-down Crab-like radio pulsars ($T_s \sim 10^3$ yr).

Between the stellar core and the world outside it there is a solid crust with a very high electrical conductivity. If the crust were absolutely rigid and a perfect conductor, then its response to changes in the core magnetic field would be limited to rigid crust rotations. Of course neither is the case.

A high density of core flux tubes merges into a smooth field when passing through the crust. Because of the almost rigid crust's high conductivity, it, at least temporarily, freezes in place the capitals of the core's flux tubes. As these flux tube capitals at the crust-core interface are pushed by a moving core neutron vortex array, a large stress builds up in the crust. This stress will be relaxed when the crust is stressed beyond its yield strength, or, if the buildup is slow enough, by dissipation of the crustal eddy currents that hold the magnetic field in place as it passes from the core through the crust. The shear modulus of a crust is well described quantitatively, but not the maximum crust strain before yielding (and the associated yield strength). Rough estimates have suggested a maximum yield strain, $\theta_{\max}$, between 10^{-4} and 10^{-3} (Ruderman 1991a, 1991b). Nor is it known how the stellar crust moves when its yield strength is exceeded. By plastic flow (creep)? By crumbling? By cracking? The answer is likely to depend on the crust temperature. A crust's eddy current dissipation time could be anywhere in the range 10^6–10^{10} yr, depending upon how the crust was made. A young solitary pulsar was probably born with a temperature $k_B T \sim 10$ MeV. As it cooled, the

formation of crust nuclei and their crystallization into a crustal lattice occurred at about the same temperature, $k_B T \sim 1$ MeV. The impurity fraction (the probability that neighboring nuclei have different proton numbers) has not been calculated quantitatively, and this allows a very wide latitude in the possible range for the "impurity" contribution to crustal resistivity. In addition, the crust of an accreting neutron star spun up to a period of a few milliseconds in a low-mass X-ray binary (LMXB) has had a very different history from that of a solitary spinning-down radio pulsar. The LMXB neutron star ultimately accretes more than 10^2 times the mass of the nuclei in its crustal lattice, mainly as He or H. Crust is continually pushed into the core by the loading, and replaced. As the accreted H and He are buried with growing density a series of nuclear reactions ultimately fuse them into heavier magic-number nuclei ($Z = 40, 50, 32$) (Negele & Vautherin 1973). This is probably not accomplished without some explosive nuclear burning. The resulting re-formed crust may well have an impurity fraction, electrical conductivity, and crust thickness very different from that of a canonical young solitary radio pulsar.

There seems to be considerable observational, as well as theoretical, support for the hypothesis that the surface magnetic fields of neutron stars slowly spun up to become millisecond pulsars by accretion in LMXBs do indeed reflect the expected core field evolution at the crust-core interface (Chen, Ruderman, & Zhu 1997; Chen & Ruderman 1993). The core field there does appear to have had a case *a* history: the core's magnetic flux tubes were moved in to the spin axis by the contracting neutron superfluid vortex array. Here the spin-up timescales ($\geq 10^8$ yr) are so very long that crustal shielding of core magnetic field changes is expected to be relatively easily defeated. Rough estimates of crust properties (Ruderman 1991a, 1991b) indicate that, generally, crustal yielding in the younger, much more rapidly spinning-down pulsars also causes the surface field of such neutron stars to be strongly correlated with the configuration of the core flux which enters the crust at the core-crust interface. (See, however, the exception for the very slowly spinning X-ray pulsars.) Stratification in the crust (because the Z of the most stable nucleus varies with depth) allows mainly only two-dimensional crustal movement on surfaces of constant gravitational (plus centrifugal) potential. Where the surface field is strongest, and crustal stresses from moving crust-anchored core flux are greatest, crustal matter would be expected to move with the core's moving flux, accompanied by the backflow of more weakly magnetized regions of the crust. Below, except for the special case of the very slow X-ray pulsars, we shall simply assume that shielding by the crust of changes in the core flux emerging into it is, at best, temporary and unimportant even on the spin-down timescales of solitary radio pulsars.

In § 3 we review the expected pulsar magnetic dipole moment evolution caused by neutron star spin-down or spin-up. It gives young radio pulsar spin-down indices which do not disagree with observations. These results are not sensitive to details of just how a crust relaxes the growing stresses on it from the moving core magnetic flux tubes below it. In § 4 we consider particular consequences when that relaxation is accomplished by large-scale crust-cracking events, which cause pulsar timing glitches. A permanent (i.e., unhealed) jump in spin-down rate should remain after almost all glitches. The calculated glitch spin-period jump magnitude is closely related to it. Both depend upon how much crust stress relaxation is accomplished in each such cracking event. This can be estimated very roughly at best. However, the glitch model does lead to predictions for the magnitudes of small glitches in Crab-like pulsars and of giant ones in Vela-like pulsars, for the intervals between such glitches, for a drop in glitch magnitudes in long-period pulsars and maximum pulsar period beyond which large glitches should disappear. These predictions are not in conflict with glitch observations. One important consequence of the model is that some parts of the core neutron superfluid can spin up very slowly after the beginning of a glitch because of the large drag in rapidly moving core vortices embedded in a dense flux-tube array. If so, the canonical assumption (Alpar & Sauls 1988) of an unobservably tight coupling between all of a core's neutron superfluid and the charged components of the pulsar should be reassessed.

2. CORE FLUX-TUBE MOVEMENTS IN PULSARS

During neutron star spin-down (e.g., in a solitary radio pulsar) or spin-up (e.g., by accretion in a low-mass X-ray binary), neutron superfluid vortices a vector distance $\boldsymbol{r}_\perp$ from the stellar spin axis move with a radial velocity

$$\boldsymbol{v}_V = -\boldsymbol{r}_\perp \dot{P}/2P \, . \tag{4}$$

As a result of this motion, a force density ($\boldsymbol{F}$) will build up on the flux-tube array in which these vortex lines are embedded until the flux tubes move with, or are cut through by, the moving vortices. The core electron-proton plasma is almost incompressible, and its abundance relative to the core neutrons varies with radius. Because of the extremely weak conversion rate for the transformations $n \rightarrow p + e + \tilde{\nu}$ and $p + e \rightarrow n + \nu$ needed to maintain a large bulk electron-proton sea transport across stellar radii, nondissipative motions in which the electron-proton plasma and its embedded flux tubes move together are restricted. We consider below mainly the alternative where flux tubes in response to the force on them from a changing neutron vortex array move through the proton-electron sea with some relative velocity $\boldsymbol{v}_\phi$.

Magnetic field movement by eddy diffusion in an ordinary conductor is driven by the self-stress force density of a non–force-free $\boldsymbol{B}$-field configuration:

$$\boldsymbol{F} = \frac{\boldsymbol{J} \times \boldsymbol{B}}{c} \, . \tag{5}$$

This $\boldsymbol{F}$ forces flux to move through the conductor with a characteristic velocity

$$\boldsymbol{v}_\Phi \sim \frac{\boldsymbol{F} c^2}{\sigma B^2} \, , \tag{6}$$

where σ is the electrical conductivity of the medium. Here the force density $\boldsymbol{F}$ is mainly a consequence of large-scale inhomogeneity in the field distribution,

$$\boldsymbol{F} = \frac{(\nabla \times \boldsymbol{B}) \times \boldsymbol{B}}{4\pi} \, . \tag{7}$$

The time for $\boldsymbol{B}$ to be pushed out of a stationary stellar core of radius R would then be the usual eddy diffusion time

$$\tau \sim \frac{R}{v_\Phi} \sim \frac{4\pi\sigma R^2}{c^2} \, . \tag{8}$$

The resistivity σ^{-1} in a nonsuperconducting degenerate electron-proton sea is dominated by electron-phonon scattering (Baym, Pethick, & Pines 1969a):

$$\sigma_{e\mathrm{ph}}^{-1} = 7 \times 10^{-46}\left(\frac{10^{13}\ \mathrm{g\ cm^{-3}}}{\rho_p}\right)^{3/2} T^2\ \mathrm{s}\ , \qquad (9)$$

where T is the temperature and ρ_p the proton density. From the resistivity of equation (9) with a plausible neutron star parameter and the $\boldsymbol{F}$ of equation (7) with $|\nabla \times \boldsymbol{B}| \sim |\boldsymbol{B}/R|$, τ greatly exceeds 10^{10} yr. The v_Φ of equation (6) would then be too small to be of interest for observable flux changes in a spinning-down (or spinning-up) neutron star. However, when the proton sea becomes superconducting, the v_Φ of equation (6) can become very much greater. This is because of the submicroscopic bunching of $\boldsymbol{B}$ into the huge density of quantized flux tubes. This has two consequences. First, a randomized electron scattering comes not only from collisions with phonons but also from collisions with the flux tubes themselves. The latter contributes a much larger resistivity than that of equation (9). Second, the contribution to the force $\boldsymbol{F}$ that drives the flux-tube motion which is caused by the push of moving superfluid neutron vortex-lines on flux tubes can very greatly exceed that of equation (7), the self-stress calculated from the large-scale variation of a classically smooth field. Flux-tube motion in response to some $\boldsymbol{F}$ is possible only if the necessary energy dissipation accompanying it equals the work done by $\boldsymbol{F}$; then

$$\boldsymbol{v}_\Phi \cdot \boldsymbol{F} = \sigma\left(\frac{\boldsymbol{v}_\Phi \cdot \hat{\boldsymbol{B}} n_\Phi \Phi_0}{c}\right)^2 + n_\Phi \eta v_\Phi^2\ , \qquad (10)$$

where the locally average field is $\boldsymbol{B} = n_\Phi \Phi_0 \hat{\boldsymbol{B}}$. The first term on the right-hand side is the dissipation from the current flow caused by the simultaneous motion of very many flux tubes. (It has typically been neglected in the literature. Its importance was emphasized by P. Goldreich 1993, private communication.). In writing equation (10) we make the implicit assumption that the original array of flux tubes moves but no new flux loops are created or existing ones reconnected and destroyed. They may not be valid except in the limit of very small v_Φ. The conductivity σ is that for (electron) current flow in the $\boldsymbol{E} = \boldsymbol{v}_\Phi \times \boldsymbol{B}/c$ direction, i.e., perpendicular to $\boldsymbol{B}$. For a given $\boldsymbol{B}$ this contribution to dissipation is not sensitive to details of flux-tube radii or the magnitude Φ_0 except through the dependence of σ upon both of them.

The second term on the right-hand side is from the direct drag force (along $\boldsymbol{v}_\Phi$) on individual flux tubes pushing through the electron sea. The drag coefficient (force per unit length of flux tube $= \eta v_\Phi$) on an isolated solitary flux tube (Jones 1987; Harvey, Ruderman, & Shaham 1986),

$$\eta = \frac{3\pi\Phi_0^2 e^2 n_e}{64\Lambda_* c E_\mathrm{F}}\ , \qquad (11)$$

where E_F is the electron-sea Fermi energy and Λ_* the radius of a flux tube ($\sim 10^{-11}$ cm). [$\Lambda_* = (m_p m_p^* c^2/4\pi e^2 \rho_p)^{1/2}$ with m_p^* the effective proton mass and ρ_p the proton plasma density.]

The electron resistivity, σ^{-1}, now has two contributions. One is the contribution from electron-phonon scattering of equation (9); the other is from scattering of electrons on the flux tubes themselves. Because the magnetic flux is bundled into intensely magnetized flux tubes at each of which electrons are scattered through a finite angle ($\Delta\Phi$), there is a drag along the electron velocity proportional to $(\Delta\Phi)^2$ at each scattering. (Equivalently, the circular trajectory of an electron in a "uniform" $\boldsymbol{B}$ is replaced by a polygon with a random scattering component $\sim[(\Delta\Phi)^2]^{1/2}$ at each vertex.) Because the separation between scatters [$\gg(\Phi_0/B)^{1/2} \sim 3 \times 10^{-10} B_{12}^{-1}$ cm) is very large compared to $\hbar c/E_f \sim 10^{-13}$ cm, there is negligible interference between scattering at different vertices.] The drag along the electron velocity is just that from equation (11). It contributes a resistivity

$$\sigma_{e\Phi}^{-1} = \frac{\eta n_\Phi}{e^2 n_e^2}\ , \qquad (12)$$

where n_e is the number density of electrons. The contribution of equation (12) to

$$\sigma^{-1} = \sigma_{e\Phi}^{-1} + \sigma_{e\mathrm{ph}}^{-1} \qquad (13)$$

is generally much more important than that of equation (9). (For typical neutron star parameters $\rho_p \sim 10^{13}$ g cm^{-3} and $T = 10^8$ K, $\sigma_{e\mathrm{ph}}^{-1} \sim 10^{-29}$ s, while $\sigma_{e\Phi}^{-1} \sim 10^{-27} B_{12}$.) If we neglect it we can approximate a very small flux-tube velocity in the direction of an $\boldsymbol{F}$ perpendicular to $\boldsymbol{B}$ by the exact analog of equation (6):

$$\boldsymbol{v}_\Phi \sim \frac{\boldsymbol{F} c^2}{\sigma n_\Phi^2 \Phi_0^2}\ , \qquad (14)$$

with an effective conductivity

$$\sigma = \left(\frac{e^2 n_e^2}{\eta} + \frac{c^2 \eta}{\Phi_0^2}\right) n_\Phi^{-1}\ . \qquad (15)$$

We note that $\boldsymbol{v}_\Phi \to 0$ when $\eta \to 0$ because of infinite electron conductivity, and also when $\eta \to \infty$ because of the infinite drag on a solitary moving (with respect to the electron-proton sea) flux tube. The contribution of the second term on the right-hand side of equation (15) to σ is generally negligible in typical pulsars.

To evaluate the maximum $|\boldsymbol{v}_\Phi|$ before the cutting through of a flux-tube array by a moving vortex array, we must now consider the maximum $\boldsymbol{F}$ just before cutting through begins. From the Appendix, this is, roughly,

$$F_\mathrm{max} \simeq \frac{\pi n_V}{8} B_\Phi B_V \Lambda_* \ln\left(\frac{\Lambda_*}{\xi}\right), \qquad (16)$$

with n_V the vortex area density of equation (2), $B_\Phi \sim \Phi_0/\pi\Lambda_*^2$ the magnetic field within a flux tube, $B_V \sim B_\Phi$ the magnetic field within a vortex line, and $\xi(<\Lambda_*)$ the Bardeen-Cooper-Schrieffer correlation length of the Cooper pairs in the superconducting proton sea. (The force density of eq. (16) greatly exceeds that from flux line curvature [Harvey et al. 1986] or flux-tube buoyancy [Muslimov & Tsygan 1985].) From equations (14), (15), and (16) the maximum velocity (v_c) with which a moving vortex array can push a flux-tube array through the electron-proton sea in which it is embedded would be

$$v_c = \beta\left(\frac{\Omega}{100}\right)\left(\frac{10^{12}\ \mathrm{G}}{B}\right)10^{-6}\ \mathrm{cm\ s^{-1}}\ , \qquad (17)$$

i.e., v_c is proportional to the ratio of vortex line density to flux-tube density. The proportionality constant, β, is independent of Ω and B but does depend upon properties of

neutron star matter below the crust:

$$\beta = 0.4 \ln\left(\frac{\Lambda_*}{\xi}\right)\left(\frac{B_V}{10^{15}\ \mathrm{G}}\right)\left(\frac{B_\Phi}{10^{15}\ \mathrm{G}}\right) \times \left(\frac{60\ \mathrm{MeV}}{E_f}\right)\left(\frac{10^{36}\ \mathrm{cm}^{-3}}{n_e}\right). \quad (18)$$

The constant β depends upon imprecise estimates of the vortex flux-tube interaction, the flux-tube spacing along moving vortex lines, the angle between local $\boldsymbol{B}$ and $\boldsymbol{\Omega}$, etc. However, the main problem with applying equations (17) and (18) to flux-tube motion may be the implicit assumption that $\boldsymbol{v}_\Phi$ is so small that n_Φ (and thus local $\boldsymbol{B}$) in it is qualitatively unaffected by the electric currents induced by the flux-tube motion, i.e., that the effect of $\boldsymbol{F}$ is only to move the preexisting flux tubes which remain locally straight and uniformly distributed. Further, the geometrical distribution and motion of flux tubes may, in reality, be quite complicated with flux tubes, the electron-proton seas, and neutron vortex lines moving together without cutting through in many regions and with vortices cutting through flux tubes in others. We emphasize that for two-dimensional motions of the electron-proton sea in the spherical layer just below the crust (the only core layer which directly affects the surface field), stratification does not restrict flux-tube crowns in the most magnetized regions from being moved by vortex push from initial positions near the spin axis all the way down to the equator during spin-down. We shall, therefore, consider equation (17) as a phenomenological one for the behavior of magnetic flux tubes in the stellar core layer just below the crust-core interface with B the pulsar dipole field strength inferred from spin-down. We take $\beta \sim 1$, about the value expected from equation (18), but even more because equation (17) then leads to a good description of various observed properties of young spinning-down radio pulsars.

The velocity v_V as a function of $r_\perp$ and v_c of equation (17) with $\beta = 1$ is sketched in Figure 1 for a Vela-like pulsar with $\Omega \simeq 100\ \mathrm{s}^{-1}$, and $B = 10^{12}$ G. For $r_\perp < r_c$ the neutron superfluid vortex expansion velocity (proportional to $r_\perp$) is slow enough to carry all flux tubes with the expanding vortex array, at least in the core layer just below the crust; flux-tube cut-through occurs for $r_\perp > r_c$. From equations (4) and (17),

$$r_c \simeq \left(\frac{T_s}{10^4\ \mathrm{yr}}\right)\left(\frac{\Omega_2}{B_{12}}\right)10^6\ \mathrm{cm}\ , \quad (19)$$

where T_s is the pulsar spin-down timescale (age). Then for $T_s\Omega_2/B_{12} \geq 10^4$ yr, i.e., for Vela-like pulsars and those much older, $r_c \geq 10^6$ cm, i.e., $r_c \geq R$ (the stellar radius), and all flux would move out with the $\boldsymbol{v}_V$ of the vortex array. For Crab-like pulsars with T_s an order of magnitude smaller than that for the Vela pulsar, most of the flux array (except that within $r_\perp \sim 10^{-1}R$ of the spin axis) would move out much more slowly than the neutron vortices. As indicated in Figure 1, however, it is not yet known how fast that cut-through flux-tube outward flow should be.

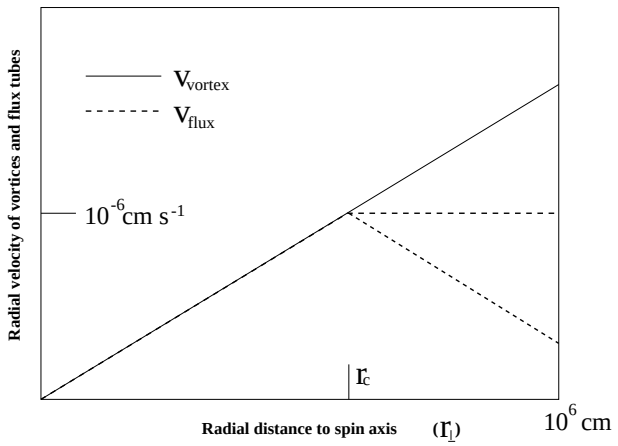

FIG. 1.—Radial vortex line speed v_V and induced flux-tube radial speed v_Φ vs. radial distance to the spin axis ($r_\perp$). For $r_\perp < r_c$, $v_\Phi = v_V$; for $r_\perp > r_c$, $v_\Phi < v_V$. It is not yet known how far v_Φ drops below v_V when $r_\perp > r_c$, and two linear possibilities are indicated.

3. SURFACE MAGNETIC FIELD EVOLUTION AND SPIN-DOWN INDICES

Based upon the above assumptions and estimates about the interaction between a pulsar core's arrays of superfluid neutron vortices and superconducting proton flux tubes, we consider below the consequences of a greatly simplified model for the evolution of magnetic fields in spinning-down pulsars:

1. The crust and core magnetic fields will be described as if they were axially symmetric around the spin axis (clearly in contradiction to what is required for a pulsar's rotating radio beams). The important consequence is that core flux tubes can then move outward only by pushing through the core's electron-proton sea, even if their actual motion is more complicated (and might not involve such push-through in many regions).

2. When $r < r_c$ of equation (19) with $\beta = 1$, flux tubes move outward with the velocity $\boldsymbol{v}_V$ of equation (4).

3. When $r > r_c$ flux tubes are moved outward with the smaller velocity v_c of equation (17). For example, in the Vela pulsar $\boldsymbol{v}_\Phi \simeq \boldsymbol{v}_V$ for almost all flux tubes, but in the Crab pulsar most flux tubes would not keep up with the core's neutron vortices. Rather,

$$\boldsymbol{v}_\Phi(\mathrm{Crab}) \sim \boldsymbol{v}_V(\mathrm{Vela})\ . \quad (20)$$

4. The surface fields of the neutron star reflect those of the core at the core-crust interface. (This, probably, would not be accomplished for exact axial symmetry. In a more realistic model it would be expected only for the most strongly magnetized regions, since some crustal backflow [where B is weakest] would be expected to allow the strongly forced crust movement where B is largest.)

We consider next a comparison of the predictions of such a model to observations of $\ddot{P}$, $\dot{P}$, and P for some of the younger pulsars. In this model the core and surface magnetic field configurations of a neutron star depend not only on the star's spin history but also on its (quite unknown) initial field configuration. It is often convenient in calculations to assume the surface field to be that of a central dipole, but there are no physical arguments supporting this special configuration as there is, for example, for the Earth's surface field where the surface is very far from the core dynamo currents. More plausible might be some (random) mixture of higher moments (Barnard & Arons 1982) or a strongly off-center dipole from a toroidal field (originally amplified by initial differential rotation) that has pushed out

through the stellar surface in some region. An initial "sunspot-like" surface field configuration seems needed to describe the evolution of some neutron stars that are spun up to become very fast millisecond pulsars (Chen & Ruderman 1993): most of the magnetic flux from each of these stars' spin-hemispheres returns to the star in the same hemisphere from which it originates.

With an axially symmetric magnetic field configuration, the spin-down rate of a solitary neutron star depends almost entirely on its net dipole moment ($\boldsymbol{\mu}$), which can vary, and its moment of inertia. The expected evolution of such a dipole moment is shown in Figure 2 together with inferred moments (from observed spin-down rates) of radio pulsars. Three common evolutionary stages are predicted for all pulsars:

Stage a–b.—In young Crab-like pulsars, r_c is much smaller than the 10^6 cm stellar radius. In most of the core, $r_\perp > r_c$. Superfluid vortices there cut through magnetic flux tubes, and $|v_\Phi| < |v_V|$. Because $\dot{\Omega} \propto \mu^2\Omega^3/Ic^2$ (essentially from dimensional arguments), with I the star's moment of inertia, the spin-down index is

$$n \equiv \frac{\ddot{\Omega}\Omega}{\dot{\Omega}^2} = 3 - T_s\left(\frac{4\dot{\mu}}{\mu} - 2\,\frac{\dot{I}}{I}\right). \tag{21}$$

Measured values of n are given in Table 1. Plausible $\dot{I}/I$ (Alpar et al. 1996) seem too small to be a promising explanation of the large $3 - n$ of Vela, and we neglect its contribution to equation (21). The model of § 2 suggests

$$\left|\frac{\dot{\mu}}{\mu}\right| \sim \frac{|v_\Phi|}{|v_V|}\,(4T_s)^{-1} \tag{22}$$

with $\dot{\mu}/\mu > 0$ for a "sunspot"-like field configuration, as long as magnetic flux has not yet been pushed out of the core at the (spin) equator. Then, for such (shorter period) pulsars,

$$3 - n \sim v_\Phi/v_V\,. \tag{23}$$

Insofar as $r_c > R$ in Vela, $v_\Phi = v_V$ for that pulsar. With this approximation the model predicts $n = 2$ for Vela. In the more general case the assumption $\dot{\Omega} \propto \mu^2\Omega^3$ is replaced by $\dot{\Omega} \propto (\alpha\mu_\perp^2 + \beta\mu_\parallel^2)\Omega^3$, where $\mu_\perp$ is the component of μ perpendicular to $\boldsymbol{\Omega}$ and $\mu_\parallel$ is the parallel component. For time-independent α and β,

$$n = 3 + \left(\beta\mu_\parallel^2 + \frac{2\beta\mu_\parallel\,\dot{\mu}_\parallel\,\Omega}{\dot{\Omega}(\alpha\mu_\perp^2 + \beta\mu_\parallel^2)} - 1\right)\frac{v_\Phi}{v_V}\,. \tag{24}$$

For a spinning dipole in a vacuum, $\beta = 0$ and equation (23) is recovered with $n = 2$ for Vela. For much more rapidly spinning Crab-like pulsars with much smaller spin-down ages, but with v_Φ still the same as that of Vela because of the cut-through of their magnetic flux tubes by their more rapidly expanding vortex arrays, the model gives

$$3 - n = (3 - n)_{\rm Vela}\left(\frac{\Omega T_s}{B}\right)\left(\frac{\Omega T_s}{B}\right)^{-1}_{\rm Vela}. \tag{25}$$

Equation (25) is used to give the other spin-down indices in the $n_{\rm model}$ column of Table 1. Comparisons with observations are satisfactory except for PSR 0540−69. However, it has been suggested (Ögelman & Hasinger 1990) that the braking index of PSR 0540−69 could be 2.7 instead of 2.0 because of a glitch just before their period measurements of this pulsar. If this is indeed the case, the agreement would be satisfactory here also. For pulsars older than 10^4 yr but not very much older, flux tubes are predicted to move outward with the same velocity as vortices. For them $|v_\Phi| \sim |v_V|$ and $n \sim 2$. (If "magnetars" [Thompson & Duncan 1993, 1995; pulsars born with huge magnetic fields ($B \sim 10^{15}$ G)] exist, they would spin down so rapidly [$P \sim 10$ s after 10^4 yr] that $v_\Phi \ll v_V$. Then for most of their early lives, $n \sim 3$ and μ would not be much diminished by the spin-down.]

Stage b–c.—Until an age $T_s \sim 10^4$ yr is exceeded, movement of the most strongly magnetized surface patches

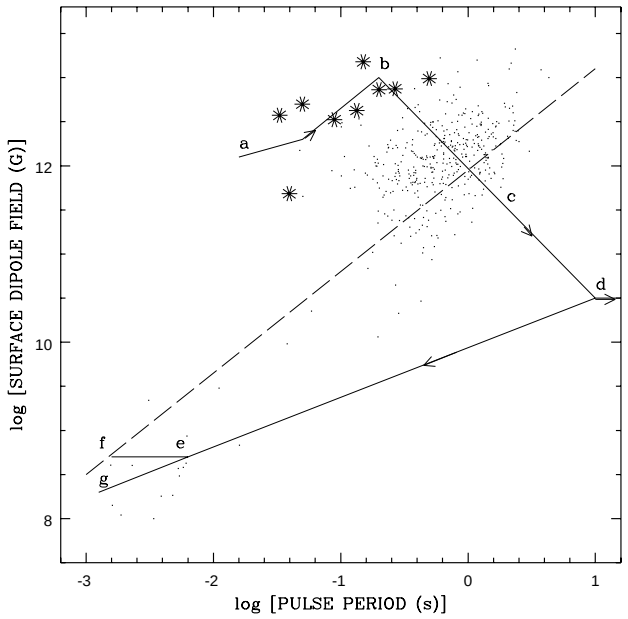

FIG. 2.—Model evolution of magnetic dipole fields of radio pulsars. Starlike designations indicate radio pulsars found in supernova remnants. In the model, solitary spinning-down radio pulsars follow the path (a–b–c). The path (a–b) corresponds to the first and second stages discussed in § 3. Spin-down follows the path (b–c–d) when field-pulled parts of the crust move toward the spin equator, where reconnection can begin after core flux expulsion. The region (d) would not be reached by a solitary pulsar, but may be by some neutron stars in binaries. Further spin-down beyond (d) would not be effective in reducing B because the crust would no longer be stressed above its yield strength. (Subsequent accretion-induced spin-up could return the neutron star to (c) if the magnetic field configuration mainly connects the two spin hemispheres.)

TABLE 1

PULSAR SPIN-DOWN INDICES

Pulsar	T_s (yr)	n	$n_{\rm model}$	Reference
Crab.....	1300	2.5	2.6	Lyne, Pritchard, & Smith 1988
PSR 1509−58.....	1500	2.8	3	Kaspi et al. 1994
PSR 0540−69.....	1700	2.0	2.7	Manchester & Peterson 1989
Vela	11000	1.4	2	Lyne et al. 1996

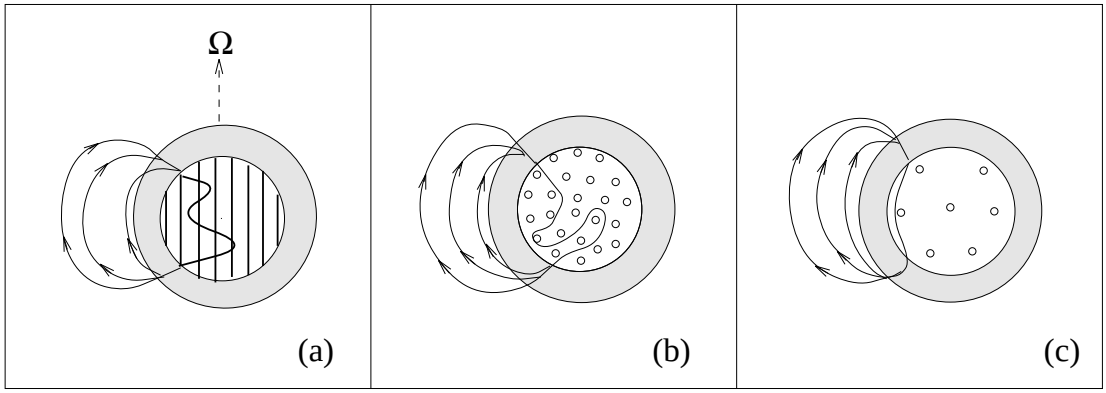

FIG. 3.—Model for movement of a single magnetic flux tube in a spinning-down neutron star core. (*a*) Side view of initial flux-tube path (*thicker line*). In the crust and beyond, the magnetic field is not confined to quantized flux tubes. Neutron superfluid vortex lines are indicated as unfilled tubes. Because the core field would be expected to have had toroidal as well as poloidal components before the superconducting transition, the flux-tube path is probably quite tortured while the vortex array is quasi-uniform. (*b*) Top view of (*a*) from along the spin-axis direction. (*c*) Top view of the flux tubes in the equatorial zone after long spin-down. A conducting crust platelet moves with the flux-tube capitals, pushed beyond the crust's yield strength in part by the crust's own pinned vortex lines and, crucially, by the pull of core flux tubes. As core neutron vortex motion moves an entrained flux tube, that tube is ultimately pushed into the crust core boundary for almost any initial flux-tube configuration.

toward the spin equator is predicted to be much slower than that of the core's neutron vortex lines. In much older pulsars, with flux tubes and vortices moving together, a significant fraction of the flux should begin to reach the spin equator and be pushed out through the crust-core interface region into the deep crust. Subsequently, the core's vortex array no longer controls the movement of that flux. The movement of a typical flux tube is sketched in Figure 3 (for an initial nonsunspot configuration). When enough flux is expelled from the core, the huge stresses that build up in the crust (whose rigidity alone prevents rapid reconnection between north and south polar regions of core-ejected flux) can become large enough to exceed the yield strength of the crust. Then reconnection allowed by crust breaking and Eddy dissipation begin. [The magnetic stress on the crust could reach or even exceed $BB_c/8\pi$, with $B_c \geq 10^{15}$ G the magnetic field within a flux tube. The yield strength of a neutron star's crust when stressed over a surface area of radius $\sim R$ is $\mu\theta_{\max}\Delta/R$, where μ is the deep crust shear modulus, Δ the crust thickness, and $\theta_{\max}$ the maximum strain before yielding by breaking or plastic flow. (This crust strength is about a tenth of the "yield stress" of crustal matter.) Because $\theta_{\max}$ depends upon uncalculated details of crustal dislocations and impurities, its value is uncertain. Typical estimates for it give $\theta_{\max} < 10^{-3}$. Then $BB_c/8\pi \sim 10^{26}$ dynes cm$^{-2} \geq \mu\theta_{\max}\Delta/R \sim 10^{25}$ dynes cm^{-2}. In addition, and perhaps of greater significance, the timescale for reconnection because of Eddy diffusion through the thin crust is diminished because of the special core-expelled magnetic field geometry: the radial field B is much smaller than the tangential field B_c. The relevant Eddy diffusion time $\sim(4\pi\Delta^2/c^2) \times$ (crust conductivity). The unknown impurity contribution to crust conductivity makes quantitative estimates of the diffusion time quite uncertain. It is not implausible that it can be less than the 10^6 yr lifetime of most radio pulsars.] The surface field evolution of a spinning-down star after most north and south pole regions reach the core's spin-equator and ultimately reconnect is sketched in Figure 4. The unreconnected flux still left in the stellar core is roughly proportional to Ω. Then $\mu \propto \Omega$, and equation (21) gives $n = 5$. This predicted decline with increasing spin period P in the dipole component of the surface field is shown as segment (b–c–d) in Figure 2. We see no reason for those strongly magnetized north and south polar surface regions (magnetized "platelets") that have been pushed to the spin equator after some fixed time to

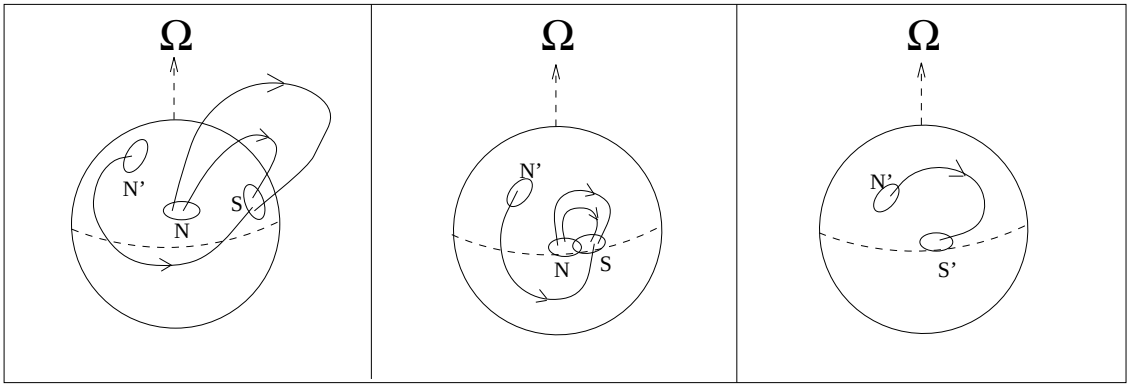

FIG. 4.—Movement of magnetized patches ("platelets") on the surface of a spinning-down pulsar: (*a*) initial surface magnetic field configuration; (*b*) after substantial spin-down, the main (most strongly magnetized) patches have reached the spin equatorial zone where reconnection can occur; (*c*) remaining magnetized patches after reconnection. The magnitude of $\boldsymbol{B}$ at the patch N′ remains about the same as its initial one in (*a*), but the dipole moment ($\boldsymbol{\mu}$) has become much smaller and its orientation is changed.

contain exactly equal amounts of flux. Any excess in the equatorial zone not canceled by reconnection would be connected to some other magnetized region that has not yet reached that zone (e.g., because it started much closer to the spin axis and therefore has moved away from it much more slowly). This is sketched as the region N′ in Figure 4. The direction of the remaining dipole $\boldsymbol{\mu}$ depends on details of the initial configuration; only its diminished magnitude is a robust prediction.Observations are not in conflict with the model curve segment b–c of Figure 2. We note especially the eight 10^4 year old radio pulsars still in supernova remnants. Unless strong μ reduction does indeed begin, similar to that indicated as segment b–c, there is a puzzle in trying to understand the Figure 2 data. Where will the descendants of these eight Vela-like pulsars in SNRs be observed ? If μ is constant, the number of pulsars in any fractional period interval $\Delta P/P$ should be proportional to P^{-2}. Thus there should then be of order 10^3 pulsars with $P \sim 1$ s with a dipole moment similar to that of these eight Vela-like pulsars. Where are they? The total number of slower pulsars actually observed does not particularly contradict this expectation, but their inferred μ is clearly diminished. With the observed $n \sim 1.4$ in Vela, this absence of a very large number of descendants of Vela-like pulsars with the same μ as that of Vela or even a greater one would be even more dramatic.

Stage c–d.—Most radio pulsars die before their spin periods exceed several seconds. However, some will be in binaries where interaction with a companion (via winds, accretion disks, common envelopes) may spin the neutron stars down to very much greater periods. The core magnetic field would continue to drop, but ultimately a lower limit would be reached where a crust's strength and high conductivity freezes the crust field even after almost all flux has been expelled from the core. Because of quantitative uncertainties about the crust's yield strength, it is not known just when this will occur. Segment d in Figure 2, where crust flux freezing is assumed to become effective, is therefore mostly a plausible guess. The magnetic moments of slow X-ray pulsars should retain such a value until crustal eddy currents decay, even though for some of them $P \sim 10^3$ s. One characteristic of the surface field of such spun-down pulsars should reflect the special way in which their dipole field was diminished. Initially separated strongly magnetized "platelets" were first pulled away from each other and, if they had opposite polarity, later had their fields reconnected after they reached the spin equatorial zone. However, each strongly magnetized platelet is much less likely to become stressed in a way that would have caused it to fragment: wherever significant field remains on the surface of a spun-down pulsar, it should still tend to have the same strong value that much of the entire stellar surface had originally. Consequently, in slowly spinning pulsars, polar cap magnetic fields measured by cyclotron resonance features in X-ray spectra should give a very considerably higher magnetic field strength than that inferred from observations which are sensitive only to the stellar magnetic dipole moment [e.g., $(P\dot{P})^{1/2}$ in radio pulsars and X-ray pulsars]. This may already be implied in observations of the accreting binary that contains the $P = 1.2$ s X-ray pulsar Her X-1. Its X-ray cyclotron resonance feature gives $B \sim 5 \times 10^{12}$ G (Trümper et al. 1978), but accretion disk modeling gives the best fit for a dipole $B \leq 10^{12}$ G (Ghosh & Lamb 1979). Stages d–e–f and d–e–g for spun-up pulsars and their relation to millisecond pulsar observations have been discussed elsewhere (Chen & Ruderman 1993; Chen et al. 1997).

4. GLITCHES

The surface magnetic field evolution in the pulsars considered above is not sensitive to details of the associated crust movements. For the warm crusts of very young radio pulsars most of the crustal stress from spin-down–induced motion of core flux should be relaxed by plastic flow ("creep"). For cooler crusts, this is no longer expected to be the case. The transition to a more brittle crust response has been estimated to be at temperatures of a few times 10^8 K (Ruderman 1991a, 1991b), about the same as that in the deep crustal layers of 10^3 year old pulsars like the Crab. In cooler spinning-down neutron stars the forced movement of the most strongly magnetized surface patches may be accomplished by large-scale crust cracking. The sudden crustal movement might itself be the cause of crustal neutron superfluid vortex line unpinning, or it might trigger a hydrodynamically supported unpinning avalanche (Alpar et al. 1993). Either mechanism would cause sudden changes in the stellar spin period that suggest various features of observed spin-period "glitches," but they seem to differ in their predictions about permanent changes in spin-down rates.

Figure 5 shows the magnitudes of the 34 glitches (sudden fractional jumps in pulsar spin frequency Ω) reported by Lyne, Pritchard, & Shemer (1995) versus the spin-down age $|\Omega/2\dot{\Omega}|$ of the glitching pulsars. Figure 6 shows their estimated "glitch activity" (the sum of all detected $\Delta\Omega/\Omega$ divided by the total observation time) as a function of pulsar spin-down age. These observed glitch activity rates support the proposal (Anderson & Itoh 1975; Alpar 1977; Alpar et al. 1984; Alpar et al. 1993; Ruderman 1976) that the main cause of the jumps in pulsar spin rate in a glitch is a sudden spin-down of the crust's internuclear neutron superfluid. Because that superfluid's vortex lines can be strongly pinned to the lattice of crust nuclei, the crust neutron superfluid may not spin down smoothly with the rest of the star. If crust neutron vortex lines move outward from the spin axis only in discrete events (glitches), sudden

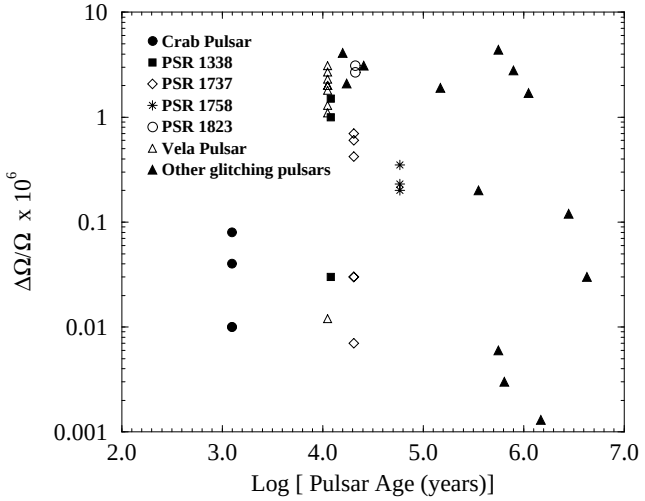

FIG. 5.—Fractional jumps in pulsar spin rate (Ω) in glitches as a function of the spin-down age ($P/2\dot{P}$) of the glitching radio pulsars (Lyne et al. 1995).

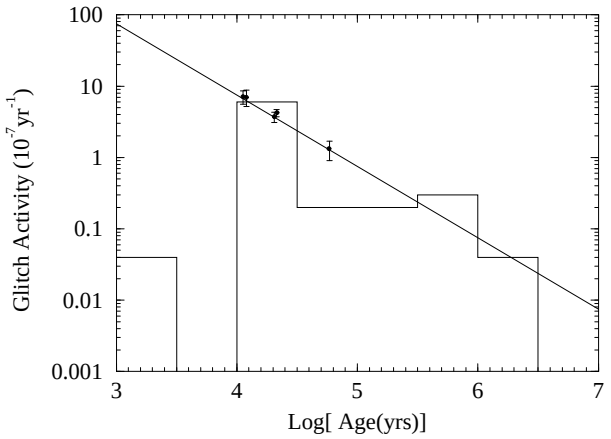

FIG. 6.—Pulsar glitch activity vs. pulsar spin age from Lyne et al. (1995). The dots are PSRs 0833, 1338, 1737, 1823, 1758. The diagonal line is the glitch activity from eq. (18) with $I_s/I_* = 1.5 \times 10^{-2}$.

spin-up glitches will be observed for the rest of the star. If these pinned vortices do not move from their pinning sites between glitches, the part of the crust superfluid neutron angular momentum ($\Delta J_{\rm csf}$) that is not diminished during the spin-down intervals between glitches (τ_g) is

$$\Delta J_{\rm csf} = I_{\rm csf}\,\dot{\Omega}\tau_g\ . \tag{26}$$

$I_{\rm csf}$ is the moment of inertia of the crustal superfluid neutrons whose spin is determined by those vortex lines which do not unpin between glitches. During one glitch or after many glitches the drop $\Delta J_{\rm csf}$ is accomplished and balanced by spin-up of the other parts of the neutron star. Then the glitch activity is

$$\frac{\Delta\Omega}{\Omega}\,\frac{1}{\tau_g} \sim \frac{I_{\rm csf}}{I_*}\,\frac{\dot{\Omega}}{\Omega}\,, \tag{27}$$

where $\Delta\Omega/\Omega$ is the observed glitch magnitude, and $I_* - I_{\rm csf}$ ($I_* \gg I_{\rm csf}$) is the moment of inertia of all the parts of the star which, before a spin-period glitch is resolved, share that angular momentum increase which balances the sudden glitch-associated decrease in the angular momentum of crust neutron superfluid. Table 2 gives the model result of equation (27) for $I_{\rm csf} \simeq 1.5 \times 10^{-2} I_*$ (a typical value of the moment of inertia of crustal neutron superfluid from neutron star models) with the glitch activity rates of those young pulsars which have been observed to glitch more than once and thus allow an estimate of their glitch activity. The comparison between equation (27) and observations is also shown in Figure 6. The agreement with equation (27) is satisfactory except for the young Crab family. The cause of this discrepancy will be discussed below.

A quantitative calculation of I_* is complicated because the core's neutron superfluid vortices are immersed in and push on the core's flux-tube array. All of the core neutron superfluid vortices would not be able to move inward quickly in response to the sudden glitch-associated spin-up of the core's electron-proton plasma (tied to the crust lattice by the strong internal magnetic field) (Ding, Cheng, & Chau 1993). It would not include the core neutron superfluid whose vortex lines would have to push flux tubes through the electron-proton sea or to cut through their surrounding flux tubes in a time too short to be observed in a glitch. I_* would then be very significantly less than the total moment of inertia of the star. The straight line in Figure 6, equation (27) with $I_{\rm csf}/I_* = 1.5 \times 10^{-2}$, fits observations except for the very young Crab-like family and the oldest pulsars ($T_s > 3 \times 10^6$ yr). If I_* were to equal the total stellar moment, this ratio gives a relatively large $I_{\rm csf}$, implying a stiff core equation of state to give a thick enough crust. On the contrary, an important softening may be a consequence of a K-meson condensate (Brown et al. 1994). In the absence of a quantitative calculation of I_*/I, which would probably also need detailed knowledge of the core's flux -tube array to support a calculation of the time history for core neutron vortex response, it may be premature to draw quantitative conclusions about neutron star structure from fits of $I_{\rm csf}/I_*$ to pulsar glitch data.

Equation (27) is not a unique consequence of any one among various glitch theories based upon the discontinuous spin-down of crust neutron superfluid. It holds, for example, as long as each crust-cracking event shakes free only some fraction of the crust neutron superfluid's pinned vortex lines, so that a typical pinned vortex line survives several glitches before it is ultimately unpinned (or even if there is no glitch vortex unpinning but only a shift in their position because of a sudden movement of the pinning sites; Ruderman 1976). It would also hold if the repeated crust neutron vortex unpinning events have a purely hydrodynamic origin and development (Alpar et al. 1993), and may well remain valid for other kinds of glitch models (Link & Epstein 1996). There are, however, other glitch observations that may discriminate among glitch models, in particular,

TABLE 2

PULSAR ACTIVITY IN YOUNG PULSARS

PULSAR	log [age (yr)]	POSTGLITCH HEALING FRACTION FOR $\Delta\Omega/\Omega$ (%)	GLITCH ACTIVITY (10^{-7} yr^{-1})	
			Observed	Eq. (27)
PSR 0531+21.....	3.10	80	0.1	62
PSR 1509−58.....	3.19	?	∼0	51
PSR 0540−69.....	3.22	?	?	47
PSR 0833−45.....	4.05	13	7	7
PSR 1338−62.....	4.08	1.1	7	7
PSR 1800−21.....	4.20	7	?	5
PSR 1706−44.....	4.24	11	?	4
PSR 1737−30.....	4.31	3	4	4
PSR 1823−13.....	4.33	7	4	4
PSR 1727−33.....	4.41	4	?	3
PSR 1758−23.....	4.77	0.1	1	1

NOTE—All data are taken from Shemar & Lyne 1996.

those which are based only on spin-up models versus models which also have glitch-associated crust-breaking displacements.

We consider below the interpretation of glitch features within the framework of the crust-cracking model in which some relaxation of the crustal stresses from core flux-tube movement is the prime cause of a glitch.

1. *The Crab pulsar's dipole magnetic field appears to jump in each major Crab glitch.*—The glitch history of the Crab pulsar is shown in Figure 7 for spin-rate changes relative to a prediction extrapolated from initial observations for P, $\dot{P}$, and $\ddot{P}$. After each of the two major glitches there is a permanent change in $\dot{P}$ indicating a crust spin-up rate change $\Delta\dot{\Omega}/\dot{\Omega} \sim 4 \times 10^{-4}$. Each repeated $\Delta\dot{\Omega}$ is much too large to be understood as coming from a plausible sudden shape change. There are two much more credible interpretations for the $\dot{\Omega}$ jumps: the spin-down torque might have suddenly increased in the glitch, or the effective crustal neutron superfluid's spin-down moment of inertia might have decreased because of some rearrangement of crustal vortex pinning (Alpar et al. 1996). This jump is a relatively huge effect; it can be seen to be very much greater than the relatively tiny $\Delta\Omega/\Omega$ of the glitch (most of which is also quickly healed). The first explanation is a natural and necessary consequence of local crust cracking causing a sudden movement of a strongly magnetized platelet. We note that the sign of $\Delta\dot{\Omega}$ would then imply a sudden, unhealed increase in the dipole moment for each major Crab glitch; this is consistent with the sign of $\dot{\mu}$ for more gradual changes inferred from the Crab spin-down index (Table 1). The presumed fractional dipole increase corresponds, roughly, to a sudden magnetized surface patch displacement (toward the equator) of $\Delta s \sim 2 \times 10^{-4} R$. This Δs does not seem implausible when compared with rough estimates of how large a healing crack displacement (if any) could be expected when the crustal yield strength is exceeded (a $\Delta s/R$ somewhat less than the maximum yield strain). We assume below that this Δs (and the associated $\Delta\dot{\Omega}/\dot{\Omega}$) value is common to all major glitches in rapidly spinning pulsars, since it depends only on the properties of a pulsar's crust, not on its period, magnetic field, or spin history. Unfortunately, it is difficult to know from present data whether or not this is the case. It is, however, not inconsistent with Vela pulsar glitch data; cf. item 2 below).

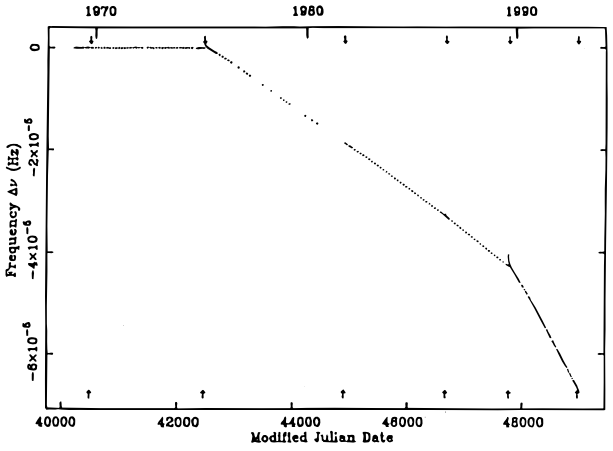

FIG. 7.—Rotation frequency of the Crab pulsar over a 23 yr period after subtracting an extrapolation from the first few years of data (Lyne et al. 1992).

2. *The glitch interval for the Vela pulsar is 3 years.*—According to equation (4), strongly magnetized platelets on Vela's crust should move toward the spin equator at an angular rate $\sim T_s^{-1}$. If this is accomplished by repeated crust-breaking glitch events a time τ_g apart, then $\tau_g \sim (\Delta s/R)T_s \sim 2$ yr. This is close to what is observed for Vela. The related question of whether there is an unhealed $\Delta\dot{\Omega}/\dot{\Omega} \sim 4 \times 10^{-4}$ in Vela after each glitch is not answered directly because, in contrast to Crab glitches, a new Vela glitch occurs before healing from the previous glitch is complete enough. However, Vela's observed 1.4 spin-down index could be interpreted solely as the consequence of an unhealed $\Delta\dot{\Omega}/\dot{\Omega} = (3 - n)/2\tau_g T_s^{-1} \sim 0.8\tau_g T_s^{-1} \sim 2 \times 10^{-4}$ after each glitch, i.e., the nearly 100% growth in magnetic moment during a spin-down time implied by $n = 1.4$ might indeed be accomplished in discrete jumps at glitches. This is not the case, however, for Crab glitches, which are too infrequent to contribute significantly to the Crab's $3 - n \sim 0.5$. We note that in the Vela-like group it would also follow from equation (27) that such glitches have a magnitude

$$\frac{\Delta\Omega}{\Omega} \sim \frac{\tau_g}{2T_s} \times 10^{-2} \sim 10^{-6}\,, \tag{28}$$

near that which is observed.

3. *The major Crab glitches are only a few times* 10^{-2} *as strong as the giant ones in the older pulsars; glitches have not been seen at all in PSR 1509−58 and PSR 0540−69.*—The defining characteristic of a glitch is the jump in the spin rate of the pulsar crust presumed to be caused by the sudden small spin-down of some crustal neutron superfluid. The crust is a layered structure. The deep crust where such vortex pinning is relevant consists of three layers, some of whose physical properties are estimated in Table 3. The nuclear charge Z of the most stable nucleus and the number density n_Z of nuclei are taken from the calculations of Negele & Vautherin (1973). In the deep crust these nuclei form a Coulomb lattice (i.e., the electron sea has a negligible polarization). The crustal lattice melting temperature (T_m) is then well approximated by $k_B T_m \sim (Ze)^2 n_Z^{1/3}/180$. The T_b column of Table 3 is 10^{-1} the calculated crust lattice melting temperature. This is about the temperature at which crystal lattices usually become brittle and yield to excessive stress by breaking instead of by plastic flow (creep) (Ruderman 1991a, 1991b). (A crust's "Coulomb lattices" have no natural scale, so that the ratio of brittle onset temperature to melting temperature should not be sensitive to density if the impurity fraction is fixed.) The last column is a very rough estimate of the moment of inertia I_{csf} of internuclear superfluid neutrons in each crustal layer relative to the moment of inertia I of the star. It is extrapolated, very roughly, from the nuclear physics calculations of Negele & Vautherin (1973)at arbitrarily selected densities by assuming that layer changes occur halfway between those densities at which there is a calculation indicating different

TABLE 3

PROPERTIES OF DEEP CRUST LAYERS

Layer	Z	T_b (K)	I_{csf}/I_{star}
a.....	32	2×10^8	$\sim 2 \times 10^{-2}$
b.....	40	3×10^8	$\sim 3 \times 10^{-3}$
c.....	50	4×10^8	$\sim 6 \times 10^{-4}$

most stable nuclei. Pinning does not exist in all of layer c, and the I_{csf} for layer c only includes the pinning part of it. The T_b are near the estimated deep crust temperatures for the 10^3 year old Crab (and for PSR 1509−58 and PSR 0540−69). As a pulsar cools, the first crust layer to become brittle (layer c) contains only $I_c/(I_a + I_b + I_c) \sim 3 \times 10^{-2}$ of the total neutron superfluid within the brittle crust of older, colder pulsars (e.g., Vela). Because the Crab pulsar would plausibly be just such a pulsar, i.e., one with a partly brittle crust, its largest glitches could be smaller by just this 3×10^{-2} ratio. PSR 1509−58 and PSR 0540−69 crusts could be sufficiently warm that their crusts are nowhere brittle enough for glitches. (Since the supernova remnant around PSR 1509−58 has an age of 20,000 yr, much longer than the pulsar's spin-down age, it has been suggested that the pulsar might have been born with a smaller magnetic field 20,000 years ago and became a pulsar only about 10^3 years ago, when its magnetic field grew to sufficient strength; Blandford, Applegate, & Hernquist 1983. However, if this is the case, this pulsar should have much stronger glitch activity. The fact that this pulsar has never been observed to glitch [Kaspi et al. 1994] is strong support for the presumption that its spin-down age is near its true age.)

4. *In addition to giant Vela-like glitches, the much weaker family of Crab-like glitches is also often observed in Vela-like and older pulsars* (Cordes 1988); *the spread in observed* $\Delta\Omega/\Omega$ *within a family is generally less than the separation between families.*—As a pulsar cools, crust magnetic stress from the pull of spin-down–induced flux-tube motion in the core is first relieved by plastic flow (PSRs 1509−58 and PSR 0540−69). At this stage there is no crust cracking and thus no glitching. In the slightly cooler Crab, crust layer c has become brittle and glitching begins in that layer. After 10^4 yr the crust is cool enough so that all three layers, a, b, and c, are brittle and we can now recognize several glitch families with relative magnitudes for $\Delta\Omega/\Omega$ proportional to the I_a, I_b, and I_c of their respective neutron superfluid moments of inertia (I_{csf} of Table 3). (This explanation makes the assumption that the shearing stress needed to slide two layers with respect to each other is less than the stress that would crack either one.)

5. *Glitch magnitudes,* $\Delta\Omega/\Omega$, *decrease with increasing pulsar period, and glitching essentially ceases at* $P = 0.7$ s *regardless of pulsar age.*—This is shown in Figure 8, where the data of Figure 5 are replotted as a function of pulsar period. (No account is taken of the reduced probability for seeing a glitch in any one pulsar or of the larger number of longer period pulsars. The one reported very small pulsar glitch (Downs 1982) beyond this cutoff is anomalous in various ways, e.g., in its postglitch healing.) From equation (27) drops in $\Delta\Omega/\Omega$ must come from decreases in τ_g/T_s. Such decreases are expected when the glitching rate is proportional to the speed of the movement through the crust of the crust-anchored moving core flux tubes. This tangential speed ($\dot{s}$) is related to the outward radial velocity of core vortex lines ($v_\perp = v_V$ of equation (4) by

$$\dot{s} = \frac{v_\perp R}{(R^2 - r_\perp^2)^{1/2}} . \tag{29}$$

Since $\tau_g \sim \Delta s/\dot{s}$, both τ_g and $\Delta\Omega/\Omega$ (from eq. [27]) approach zero as the core's flux tubes reach the core radius at $r_\perp = R$. However, a more quantitative calculation of the $r_\perp$ at which

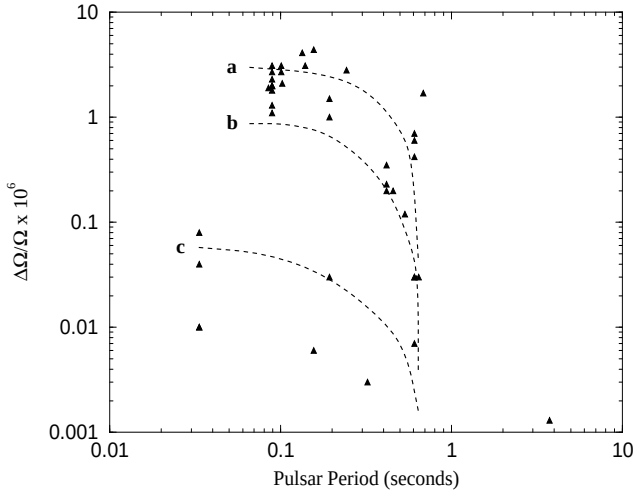

FIG. 8.—Observed glitch magnitudes (Lyne et al. 1995) vs. pulsar period.

glitching should stop must not ignore the finite yield strength of the crust. Because of it, crust yielding as well as glitching should cease somewhat before $r_\perp = R$ is reached.The three dashed curves of Figure 8 are the predicted $\Delta\Omega/\Omega$ from equation (27) and equation (29) for the three deep crust layers of Table 3 with their different I_{sfn}. The $r_\perp$ are related to pulsar spin periods by

$$r_\perp = r_\perp(0)\left(\frac{P}{P_0}\right)^{1/2} , \tag{30}$$

where $r_\perp(0)$ is the distance from the spin axis of the most important magnetized surface platelets when the spin period $P = P_0$. The plotted curves are for $r_\perp = r_\perp(0) = 0.4R$ when $P = P_0 = 0.1$ s; P_0 is the spin period of the Vela pulsar family, where $v_\Phi \sim v_V$ is finally achieved and $r_\perp(0)$ is taken as a plausible estimate. [An $r_\perp(0)$ of order $R/2$ corresponds to $P \sim 0.5$ s for canonical large glitch cessation.) The magnitude of the giant glitches in Vela is determined by using the assumed pulsar- and glitch-independent $\Delta s \sim 2 \times 10^2$ cm crust displacement in Crab glitches together with the (calculated) ratio of the crust superfluid moment of inertia to $I_* \sim I$. The smaller glitch magnitudes are then fixed by the relative moments $I_{a,b,c}$. The fits of the model curves in Figure 8 seem suggestive of present glitch data.

6. *Crab glitches occur at intervals larger than those between Vela glitches* (3 yr).— Most models predict (in agreement with observations of other glitching pulsars) that the glitching rate is roughly proportional to a pulsar's spin-down rate. This would imply that the Crab should glitch at almost 10 times the rate for Vela. However, in the model of § 2, the glitch rate determined by core flux-tube movement is proportional only to the core flux array expansion velocity. It will no longer be proportional to the spin-down rate when superfluid neutron vortices cut through core flux tubes, as is expected to be the case for the Crab pulsar (cf. Fig. 1). Rather,

$$\tau_g \sim \frac{4T_s \Delta s}{R} \frac{|\boldsymbol{v}_V|}{|\boldsymbol{v}_\Phi|} . \tag{31}$$

With $|\boldsymbol{v}_\Phi|/|\boldsymbol{v}_V| \sim 0.2$ for the Crab pulsar and ~ 0.8 for the Vela pulsar so that equation (23) gives the observed spin-

down indices, the predicted $\tau_g(\text{Crab}) \sim 0.4\tau_g(\text{Vela})$. This only partly accounts for the long τ_g(Crab). Another contribution to increasing it might come from some plastic flow to release stress in the mainly brittle layer c. It thus appears that there are two separate reasons for the greatly diminished glitch activity of the Crab pulsar family, a restricted (or absent) brittle layer that leads to very small $\Delta\Omega/\Omega$, and a cutting-through of flux tubes by vortex lines that extends τ_g.

7. *At least one Crab pulsar glitch has a resolvable initial rise in spin rate* (Lyne, Smith, & Pritchard 1992; Lyne, Pritchard, & Smith 1993). After any sudden motion of the crust there can be some glitchlike spin-up even in the absence of any spin-down of crustal neutron superfluid. The positions of vortices in the expanding core vortex array are determined by a balance between the Magnus forces which push the vortices outward and the 10^{15} flux tubes per vortex line which encompass each of them and restrain their outward movement. These flux tubes are anchored by the quasi-rigid highly conducting crust. Wherever that crust breaks to relax some of the resulting stress, the restraining forces on the vortices are diminished and the vortices may move outward to new positions. How quickly they will do this is still unclear (cf. § 2) and may differ greatly among the superfluid regions. When the new steady state is finally accomplished, there is an increase in Ω, the spin of the rest of the star, of roughly

$$\frac{\Delta\Omega}{\Omega} \sim \frac{\Sigma_{\max} I_n'}{I\rho_n R^2\Omega^2}\left(\frac{l}{R}\right)\left(\frac{\Delta s}{R}\right), \tag{32}$$

where $\Sigma_{\max}$ is the yield stress of crustal matter, l is the crust thickness, Δs is the crust shift in a cracking event (§ 4, interpretation 1), and I_n' is the moment of inertia of those core neutrons whose spin-down decrement is fast enough to contribute to a glitch observation. For a typically assumed $\Sigma_{\max} \sim 10^{26}$ dynes cm^{-2} (corresponding to a yield strain $\sim 3 \times 10^{-4}$), and $\Delta s \sim 10^2$ cm from § 4, interpretation 1,

$$\frac{\Delta\Omega}{\Omega} \sim \frac{10^{-9} I_n'}{\Omega_2^2 I}. \tag{33}$$

This is too small and has the wrong Ω dependence to be a significant addition to the $\Delta\Omega/\Omega$ of giant glitches, but it may be significant for the Crab-like glitch family. It would differ in its initial time dependence from that expected from sudden crustal vortex unpinning: instead of an initial (still unresolved) spin-down as angular momentum is transferred to core neutrons, there would be an initial spin-up as angular momentum flows in the opposite directions. This may be suggestive of the Crab 1989 glitch, but more observations and analyses of the beginning of a Crab-like glitch are needed.

5. PROBLEMS

In this section we discuss special problems associated with the proposed model that need further investigation. The first is that the total heat generation predicted by the simplified version of the model seems too large compared to the upper bound to it from X-ray observations; the second is that the timescale for angular momentum sharing between neutron star crust and some of its core neutrons given by the model seems very much longer than the conventional irresolvably short one used in glitch analyses (e.g., Alpar & Sauls 1988).

5.1. *Heat Generation during Neutron Star Spin-down*

To move outward during spin-down, core vortex lines must either push flux tubes through the core electron-proton sea or cut through them. Either would generate heat that must be compared to bounds on it from thermal X-ray observations of pulsars. When there is no flux-tube cutting and all flux tubes are pushed through a core's stationary electron-proton sea, the heat production rate would be

$$\dot{Q} = \int \boldsymbol{F} \cdot \boldsymbol{v}_{\Phi}\, d^3r \sim \frac{\pi\sigma B^2 R^5}{30c^2 T_s^2}$$

$$\sim 10^{35}\left(\frac{B}{10^{12}\text{ G}}\right)\left(\frac{R}{10^6\text{ cm}}\right)^5\left(\frac{10^4\text{ yr}}{T_s}\right)^2 \text{ ergs s}^{-1}. \tag{34}$$

But soft X-ray observations of Vela seem to give a bound of $\dot{Q} \simeq 10^{33}$ergs s^{-1} (Ögelman, Finley, & Zimmerman 1993). This large discrepancy suggests that understanding how moving core vortex lines move with, or through, the extraordinarily dense flux-tube array in which they are embedded, without an unacceptably large $\dot{Q}$, may be an important question for almost all spin-down models of strongly magnetized pulsars. Below we list various possibilities for resolving this problem while still preserving essential features of the model proposed in § 2.

1. A most obvious failure of the idealized model is its (obviously false) assumption that the core magnetic field of a pulsar can be approximated as one with enough axial symmetry around $\boldsymbol{\Omega}$ so that outward-moving flux tubes must always move through the electron-proton sea in which they are embedded. However, this is probably not at all the case in regions with inhomogeneously distributed strong core magnetic flux densities. Magnetic flux tube, vortex lines and electron-proton plasma might all move together, where n_{Φ} is very large without heat generation. In that case the integration volume of equation (34) and the relevant B^2 could be much smaller.

2. In equation (34) it has been assumed that vortices are moving together with flux tubes everywhere in the core. This might not hold for the Vela pulsar. If the critical radius of equation (19) is only, say, about one-third of the radius of the Vela pulsar core, the average velocity of flux tubes would be roughly 3 times smaller than that of vortices and the total heat generated could be almost an order of magnitude smaller.

3. A key assumption of the analysis of flux-tube drag in being pushed through the electron-proton sea plasma is that magnetic flux tubes are relatively uniformly distributed at least on the microscopic level. If this is not the case and some clumping instabilities among flux tubes develop during spin-down, the drag force on the moving flux tubes could be much smaller and thus give smaller heat generation. Flux tubes may tend to clump around the moving vortex lines (about 10^{-2} cm away from each other), while electron-proton backflow occurs in between, where there are almost no flux tubes. As in item 1 above, a relative motion between flux tubes and the electron-proton sea could be restricted to very weak B-field regions.

4. A type I superconductor might be formed by protons in most of a neutron star core. From an estimate of the core proton gap energy of $\Delta \sim 1$ MeV, it had been argued (e.g., Baym et al. 1969a) that core protons form a type II superconductor. However, a subsequent calculation (Wambach, Ainsworth, & Pines 1990) which took account of the

nuclear interaction between protons and neutrons gave a much smaller gap energy ($\Delta \sim 0.2$–0.3 MeV). It is then somewhat less clear whether the core protons form a type II or a type I superconductor. For a stiff equation of state, part of the core protons may well form a type I superconductor, while for a soft equation of state it is probable that only the type II superconductor exists in the core protons of a neutron star. Evidence supporting an intermediately stiff or a stiff equation of state (Link, Epstein, & Van Riper 1992) suggests that protons might indeed form a type I superconductor in part of the core. There, magnetic field would be in a mixed state in which B becomes large enough ($\sim 10^{15}$ G) to quench superconductivity in some small slablike regions, and essentially vanishes in between them. The typical size of such field-free regions is about $(L\xi)^{1/2}B_c/B \sim 1$ cm, with $L \sim 10^6$ cm the assumed scale size of the type I superconducting region. The type I region can also influence flux tubes in a type II region to bunch together on a similar 1 cm scale. This could significantly reduce drag forces and thus $\dot{Q}$.

5. Some $\dot{Q}$ might escape from the star's near environment as hard unobserved UV that the soft X-ray observation bound for $\dot{Q}$ is significantly exceeded. In young γ-ray pulsars such as Vela there are plausible mechanisms for the generation of $e^{\pm}$ clouds all around the near environment of the pulsar. Because of the huge e^+/e^- cyclotron resonant scattering of X-ray photons of energy $e\hbar B/mc$, an energy which extends from 20 keV to 20 eV within 10 stellar radii, this $e^{\pm}$ atmosphere would be optically thick to thermal X-rays for plausible $e^{\pm}$ densities (Zhu & Ruderman 1997). Much of the emitted soft X-rays might then be degraded to hard UV before escaping through this magnetized lepton "blanket."

Among all of the above possibilities, the first would appear most likely to be important, i.e., a fundamental inadequacy of the idealized model for core flux-tube motion (especially in layers not adjacent to the crust-core interface).

5.2. *The Initial Glitch Timescale*

The timescale ($\tau_{\text{spin-up}}$) for a suddenly spun-up crust, in a glitch, sharing its tiny angular momentum jump with the core's much heavier superfluid neutrons is usually taken to be unobservably short (Alpar et al. 1993). Because it is not resolved in the Vela pulsar, this timescale is presumed to be less than 10^2 s (McCulloch et al. 1990; Flanagan 1990). The value estimated from our proposed model or any model which involves flux-tube drag or cutting through can give a very different result. Because of the drag on the 10^{14} flux tubes that must be carried inward or cut through by each of Vela's core vortex lines to accomplish a small rapid increase in core neutron angular rotation speed, the response of these superfluid neutrons may be very sluggish.

For Vela's core superfluid neutrons to share very quickly in the angular momentum given up by crustal superfluid neutrons in a glitch, the core neutrons' vortices must move inward about 1 cm in less than 10^2 s. Before this occurs, the core vortex array first increases its rotational speed in response to the sudden spin-up of the core's flux tubes with which these vortices interact. This causes an incremental inward push (Magnus force) on the core neutron vortices. This force density,

$$\delta F \sim n_r \frac{\pi\hbar}{m_n} \rho_n \delta\Omega R = \delta\Omega\Omega\rho_n R \,, \tag{35}$$

where $\delta\Omega \sim 10^{-4}\Omega$ is the initial (unresolved) giant glitch spin-up before there is any transfer of angular momentum to core superfluid neutrons. If the subsequent inward vortex motion involves pushing flux tubes through the electron-proton sea, equation (14) gives a maximum inward flux tube speed

$$\delta v_\Phi \sim \frac{\delta\Omega\Omega\rho_n Rc^2}{\sigma n_\Phi \Phi_0^2} \sim 10^{-11} \text{ cm s}^{-1} \,. \tag{36}$$

To move inward by 1 cm would then take

$$\tau'_{\text{spin-up}} \sim 10^{11} \text{ s} \sim T_s \,. \tag{37}$$

Where flux-tube cut-through by moving vortices occurs first, the timescale $\tau'_{\text{spin-up}} \gg 10^2$ s for $B \sim 10^{12}$ G (Ding et al. 1993). Almost all of the possibilities in § 5.1 for reducing $\dot{Q}$ would also reduce $\tau_{\text{spin-up}}$, but for some, or perhaps all, core neutrons the needed reduction seems so large that it is hard to see how $\tau_{\text{spin-up}}$ can become unobservably short for all of the core neutron superfluid. One possibility for resolving this problem may be to accept the model result that where vortices must push flux tubes through the electron-proton sea or cut through them, $\tau_{\text{spin-up}}$ is unresolved because it is too long, i.e., far longer than the interval between glitches (τ_g). With the possible resolution suggested in § 5.1, possibility 1), those vortex lines whose surrounding flux tubes move with their embedding electron-proton sea may quickly adjust ($\tau_{\text{spin-up}} < 10^2$ s) and also generate little $\dot{Q}$, while only a very small minority of vortex lines with the flux tubes they carry actually move through their local charged sea. If this is the case, although the I_* of equation (27) would not include all core superfluid neutrons, it still might be nearly the entire I of the star. This would also be the case if the core is mainly a K-condensate or quark matter, superconductors with no purely neutral superfluids to be spun up in a glitch. (The charged ones are easily spun up by any magnetic field that couples them to the crust.) It should be noted that a large reduction of $\tau_{\text{spin-up}}$ for some parts of the core neutron superfluid could put the timescale in the range where it should contribute to glitch "healing" analyses.

It is a pleasure to thank A. Alpar, K. S Cheng, P. Goldreich, F. Graham-Smith, A. Lyne, and D. Pines for informative conversations. This work was supported in part by NASA grant NAG 5-2016.

APPENDIX A

SUPERFLUID-SUPERCONDUCTOR INTERACTIONS

Because magnetic fields inside neutron stars are usually not aligned along the spin axis when neutron stars spin down (up), the outward- (inward-) moving superfluid neutron vortices run into proton flux tubes. The interaction between superfluid neutron vortices and proton superconductor magnetic flux tubes as they try to cross through each other can thus play an

important part in determining the motion of both vortices and flux tubes. Srinivasan et al. (1990) proposed that the proton density perturbation in the center of a flux tube would give rise to an interaction energy per intersection

$$E_{\rm int} \sim n_n \frac{\Delta_p^2}{E_{F_p}^2} \frac{\Delta_n^2}{E_{F_n}} (\xi_n^2 \xi_p) \simeq 0.1 \text{ MeV} , \tag{A1}$$

where $\xi_{n,p}$ are the neutron, proton BCS correlation lengths, $\Delta_{p,n}$ are the respective gap energies, $E_{F_{p,n}}$ the Fermi energies, and n_n the neutron number density. An even more important contribution to the interaction energy comes from the magnetic interaction between neutron vortex lines and proton flux tubes and from the velocity dependence of the nuclear interaction between the neutrons in a vortex and the protons in a flux tube, which is also the ultimate cause of the neutron vortex line flux. Both can be taken into account using an effective Ginzburg-Landau (GL) free energy ($f_{\rm GL}$) for an interacting mixture of superfluid neutrons and superconducting neutrons (Alpar, Langer, & Sauls 1984):

$$f_{\rm GL} = f_u + \frac{1}{2} \rho_s^{pp} v_p^2 + \frac{1}{2} \rho_s^{nn} v_n^2 + \rho_s^{pn} \boldsymbol{v}_p \cdot \boldsymbol{v}_n + \frac{B^2}{8\pi} , \tag{A2}$$

where f_u is the condensation energy density, ρ_s^{pp} and ρ_s^{nn} are the "bare" densities of superconducting protons and superfluid neutrons, respectively, ρ_s^{pn} is the coupling density, and $\boldsymbol{v}_p$ and $\boldsymbol{v}_n$ are the superfluid velocities defined by

$$\boldsymbol{v}_p = \frac{\hbar}{2m_p} \nabla\chi_p - \frac{e}{m_p c} \boldsymbol{A} , \tag{A3}$$

$$\boldsymbol{v}_n = \frac{\hbar}{2m_n} \nabla\chi_n . \tag{A4}$$

The superfluid electric current is

$$\boldsymbol{j}_s \equiv \frac{c}{4\pi} (\nabla \times \boldsymbol{B}) = \frac{e}{m_p} [\rho_s^{pp} \boldsymbol{v}_p + \rho_s^{pn} \boldsymbol{v}_n] . \tag{A5}$$

From equations (A5), and (A3) and (A4), we obtain London's equation,

$$\nabla^2 \boldsymbol{A} - \frac{\boldsymbol{A}}{\Lambda_*^2} = -\frac{2\pi e\hbar}{m_p^2 c} \left[\rho_s^{pp} \nabla\chi_p + \rho_s^{pn} \frac{m_p}{m_n} \nabla\chi_n \right] , \tag{A6}$$

with $\Lambda_* = (m_p^2 c^2 / 4\pi e^2 \rho_s^{pp})^{1/2}$ the effective London penetration depth. For a pure proton flux tube with $\nabla\chi_p = \hat{\phi}/r$ and $\nabla\chi_n = 0$, the above equations give

$$\boldsymbol{v}_n = 0 , \tag{A7}$$

$$\boldsymbol{v}_p = \frac{m_p}{\rho_s^{pp} e} \frac{c}{8\pi\Lambda_*} \frac{\Phi_0}{\pi\Lambda_*^2} K_1\left(\frac{r}{\Lambda_*}\right) , \tag{A8}$$

$$B = \frac{\Phi_0}{2\pi\Lambda_*^2} K_0\left(\frac{r}{\Lambda_*}\right) , \tag{A9}$$

where $\Phi_0 = \pi\hbar c/e$ is the flux quantum and K_0 and K_1 are Bessel functions of order 0 and 1 with imaginary argument. The solutions for a pure neutron vortex line with $\nabla\chi_p = 0$ and $\nabla\chi_n = \hat{\phi}/r$ or a superposition of a neutron vortex line and a proton flux tube with $\nabla\chi_p = \hat{\phi}/r$ and $\nabla\chi_n = \hat{\phi}/r$ can be obtained similarly.

$$\boldsymbol{v}_n = \frac{\hbar}{2m_n} \frac{\hat{\phi}}{r} , \tag{A10}$$

$$\boldsymbol{v}_p = \frac{m_p}{\rho_s^{pp} e} \frac{c}{8\pi\Lambda_*} \frac{\Phi_*}{\pi\Lambda_*^2} K_1\left(\frac{r}{\Lambda_*}\right) - \frac{\hbar\rho_s^{pn}}{2m_n \rho_s^{pp}} \frac{\hat{\phi}}{r} , \tag{A11}$$

$$B = \frac{\Phi_*}{2\pi\Lambda_*^2} K_0\left(\frac{r}{\Lambda_*}\right) , \tag{A12}$$

with Φ_* the total flux in a single flux tube. For an isolated neutron vortex line $\Phi_* = \Phi_0(m_p \rho_s^{pn}/m_n \rho_s^{pp})$. For a superimposed vortex line and flux tube $\Phi_* = \Phi_0(1 + m_p \rho_s^{pn}/m_n \rho_s^{pp})$.

The energy for each case can be estimated from equation (A2). The extra energy (per unit length) of the superposition of a flux tube and a vortex line relative to a distantly separated flux tube and a vortex line is

$$E \simeq \frac{\pi}{8} \left(\frac{\Phi_0}{\pi\Lambda_*^2}\right)^2 \Lambda_*^2 \frac{m_p}{m_n} \frac{\rho_s^{pn}}{\rho_s^{pp}} \ln\left(\frac{\Lambda_*}{\xi}\right) . \tag{A13}$$

There are many more flux tubes than vortices. We assume that just before cutting through, the typical distance between two consecutive flux tubes pushed by the same moving vortex is about Λ_*, i.e., flux tubes are swept up by a moving vortex but not

cut through. The magnetic repulsion between flux tubes limits their density. This repulsion is not effective until the inter–flux-tube separation approaches Λ_*. Then the maximum force density on a flux-tube array would be roughly estimated as E/Λ_*, or

$$F_{\max} \simeq \frac{\pi n_V}{8}\left(\frac{\Phi_0}{\pi\Lambda_*^2}\right)^2 \Lambda_* \frac{m_p}{m_n}\frac{\rho_s^{pn}}{\rho_s^{pp}} \ln\left(\frac{\Lambda_*}{\xi}\right) = \frac{\pi n_V}{8} B_V B_\Phi \lambda_* \ln\left(\frac{\Lambda_*}{\xi}\right), \tag{A14}$$

with n_V the number density of vortex lines, $B_\Phi = \Phi_0/\pi\Lambda_*^2$ the characteristic magnetic field in the cores of flux tubes, and $B_V = (\Phi_0/\pi\Lambda_*^2)(m_p\,\rho_s^{pn}/m_n\,\rho_s^{pp})$ the field within the cores of neutron vortex lines that are embedded in the stellar core's superconducting proton sea.

REFERENCES

Alpar, M. A. 1977, ApJ, 213, 527
Alpar, M., Anderson, P., Pines, D., & Shaham, J. 1984, ApJ, 278, 791
Alpar, M., Chau, H. F., Chang, K. S., & Pines, D. 1993, ApJ, 409, 345
———. 1996, ApJ, 459, 706
Alpar, M. A., Langer, S. A., & Sauls, J. A., 1984, ApJ, 282, 433
Alpar, M. A., & Sauls, J. A. 1988, ApJ, 327,723
Anderson, P. W., & Itoh, N. 1975, Nature, 256, 25
Barnard, J., & Arons, J. 1982, ApJ, 254, 713
Baym, G., Pethick, C. J., & Pines, D. 1969, Nature, 224, 674
Blandford, R. D., Applegate, J. H., & Hernquist, L. 1983, MNRAS, 204, 1025
Brown, G. E., Lee, C. H., Rho, M., & Thorsson, V. 1994, Nucl. Phys. A, 567, 937
Chao, N. C., Clark, J. W., & Yang, C. H. 1972, Nucl. Phys. A, 179, 320
Chen, K., & Ruderman, M. A. 1993, ApJ, 408, 179
Chen, K., Ruderman, M. A., & Zhu, T. 1997, ApJ, submitted
Cordes, J. M. 1988, ApJ, 330, 847
Ding, K. Y., Cheng, K. S., & Chau, H. F. 1993, ApJ, 408, 167
Downs, G. S. 1982, ApJ, 257, L67
Flanagan, C. S. 1990, Nature, 345, 416
Ghosh, P., & Lamb, F. 1979, ApJ, 234, 296
Harvey, J. A., Ruderman, M. A., & Shaham, J. 1986, Phys. Rev. D, 33, 2084
Jones, P. B. 1987, MNRAS, 228, 513
Kaspi, V. M., Manchester, R. N., Siegman, B., Johnston, S., & Lyne, A. G. 1994, ApJ, 422, L83
Link, B., & Epstein, R. 1996, ApJ, 457, 844
Link, B., Epstein, R. I., & Van Riper, K. A. 1992, Nature, 359, 616
Lyne, A. G., Pritchard, R. S., & Shemer, S. 1995, J. Astrophys. Astron., 16, 179
Lyne, A. G., Pritchard, R. S., & Smith, F. G. 1988, MNRAS, 233, 667
———. 1993, MNRAS, 265, 1003
Lyne, A. G., Pritchard, R. S., Smith, F. G., & Camilo, F. 1996, Nature, 381, 497
Lyne, A. G., Smith, F. G., & Pritchard, R. S. 1992, Nature, 359, 706
Manchester, R., & Peterson, B. 1989, ApJ, 342, L23
McCulloch, P., Hamilton, P., McConnell, D., & King, E. 1990, Nature, 346, 822
Muslimov, A. G., & Tsygan, A. I. 1985, Ap&SS, 115, 43
Negele, J., & Vautherin, D. 1973, Nucl. Phys. A, 207, 298
Ögelman, H., Finley, J. P., & Zimmerman, H. U. 1993, Nature, 361, 136
Ögelman, H., & Hasinger, G. 1990, ApJ, 353, L21
Ruderman, M. A. 1976, ApJ, 203, 213
———. 1991a, ApJ, 366, 261
———. 1991b, ApJ, 382, 587
Sauls, J. A. 1989, in Timing Neutron Stars, ed. H. Ögelman & E. van den Heuvel (Dordrecht: Kluwer), 457
Shemar, S. L., & Lyne, A. G. 1996, MNRAS, 282, 677
Srinivasan, G., Bhattacharya, D., Muslimov, A., & Tsygan, A. 1990, Current Sci., 59, 31
Thompson, C., & Duncan, R. 1993, ApJ, 408, 194
———. 1995, MNRAS, 275, 255
Trümper, J., Pietsch, W., Reppin, C., Voges, W., Staubert, R., & Kendziorra, E. 1978, ApJ, 219, L105
Wambach, J., Ainsworth, T. L., & Pines, D. 1990, in Proc. Neutron Stars: Theory and Observation, ed. J. Ventura & D. Pines (NATO ASI Ser; Dordrecht: Kluwer)
Zhu, T., & Ruderman, M. 1997, ApJ, 478, 701